Automatic Detection of Renal Rejection after Kidney Transplantation

Seniha E. Yuksel[1], Ayman El-Baz [1], Aly A. Farag[1]
Mohamed E. Abo El-Ghar[2], Tarek A. Eldiasty[2], Mohamed A. Ghoneim[2]

[1]*Computer Vision and Image Processing Lab, University of Louisville, Louisville, KY 40292, USA.*
{ esen, elbaz, farag }cvip.louisville.edu, www.cvip.uofl.edu
[2]*Mansoura University, Urology and Nephrology Center, Mansoura, Egypt*

Abstract

Acute rejection is the most important reason of graft failure after kidney transplantation, and early detection is crucial to survive the kidney function. Dynamic Contrast Enhanced Magnetic Resonance Imaging (DCE-MRI) is an imaging modality where a contrast agent (such as Gd-DTPA) is introduced into the kidney and rapid and repeated images are taken, which allows both the anatomic and functional information of the kidney to be monitored. Using these images, this paper introduces an accurate method for the segmentation of the kidney from the surrounding structures by introducing a shape model of the kidney into the external energy component of the deformable models. Secondly, registration algorithms are employed to account for the motion of the kidney due to patient breathing and finally, the perfusion curves obtained from the cortex that show the transportation of the contrast agent into the tissue are given for future classification of normal and acute rejection transplants. Applications of the proposed algorithms yields promising results.

Key words: Dynamic MRI, kidney transplantation, renal rejection, deformable models, mutual information, contrast agents, Gd-DTPA

1. INTRODUCTION

Kidney is the most important organ for urine formation, and during urine formation, it handles several functions such as regulation of the pH, elimination of the metabolic wastes (urea, uric acid, creatinine, ammonia), conservation of important products such as amino acids and secretion of renin enzyme - a major enzyme related to the chemical reactions that control blood pressure [1].

The condition of 15% or less kidney function is called chronic kidney failure or end-stage renal disease (ESRD). At the end-stage renal disease, both kidneys are almost stopped, so the body fills up with extra fluid and wastes that would normally be filtered out. For the patients at this stage, renal transplantation has become a well-accepted treatment method, and in the United States, approximately 12000 renal transplants are performed annually [2]. However, acute rejection - the immunological response of the human immune system to the foreign kidney - is the most important cause of graft failure after renal transplantation [3], and the differential diagnosis of acute transplant dysfunction remains a difficult clinical problem.

Currently, the diagnosis of rejection is done via biopsy, but biopsy has the downside effect of subjecting patients to risks like bleeding and infections. Moreover, the relatively small needle biopsies may lead to over or underestimation of the extent of inflammation in the entire graft [4]. Therefore, a noninvasive and repeatable technique is not only helpful but also needed in diagnosis of acute renal rejection. Previous studies have shown that as the rejection develops, transplanted kidneys show a noticeable increase in size and develop abnormal flow patterns that are not uniformly distributed throughout the whole kidney [5]. Quantification of these changes can be used to detect rejections via image analysis, thus replacing risky biopsy procedures.

For this purpose, detection of acute renal rejection after kidney transplantations has become an ongoing collaboration between the University of Mansoura and the CVIP Lab at the University of Louisville. In this collaborative research, 50 kidney transplant recipients, 19 women and 31 men (mean age 39 years; range 16-55ys) are being evaluated using Ultrasound and Dynamic Contrast-Enhanced Magnetic Resonance Imaging (DCE-MRI) as well as the other routine tests. After transplantation, the abdomen is imaged daily using Color and Power Doppler Ultrasonography, and two weeks after the transplantation, DCE-MRI is performed just before biopsy to be able to measure the glomerular filtration rate (GFR) of each kidney separately. This paper mainly focuses on the DCE-MRI findings of this collaboration.

2. PREVIOUS STUDIES

Making use of the very high blood flow property of the kidney, Scintigraphy (Nuclear Imaging), DCE-MRI, Color and Power Doppler Ultrasonography modalities have been applied for renal imaging. Scintigraphy, the traditional method in renal imaging, does not give anatomical information of the kidney, i.e, the medulla and the cortex structures of the kidney cannot be separated. Ultrasonography is limited with the operators' skills, gives poor resolution for the small structures, it cannot accurately assess obese people and the examination of some structures can be hindered by the bowel gas, but has the advantage of being portable, and gives accurate measurements of size, volume and blood flow velocities [1]. On the other hand, DCE-MRI is a powerful imaging technique since it provides both functional and anatomical information, and the FDA approved contrast agent Gd-DTPA is freely filtered and not reabsorbed or secreted by the kidney [6].

However, even with an imaging technique like DCE-MRI, there are several problems. In DCE-MRI, the abdomen is scanned repeatedly and rapidly after the injection of the contrast agent; therefore, (i) the spatial resolution of the dynamic MR images is low, (ii) the images suffer from the motion induced by the breathing patient which necessitates advanced registration techniques, (iii) the intensity of the kidney changes non-uniformly as the contrast agent perfuse into the cortex which complicates the segmentation procedures. To the best of our knowledge, there has been limited work on the dynamic MRI to overcome the problems of registration and segmentation. For the registration problem, Giele et al. [7] introduced a phase difference movement detection method to correct kidney displacements, Yim et al. [8] introduced a semi-automatic contour registration method and Gerig et al. [9] proposed an image processing system using model-based segmentation. These three studies require building a mask manually by drawing the kidney contours on a 2D dMRI image, followed by the registration of the time frames to this mask. The multi-step registration approach introduced by Sun et al. [10] used local gradient and region information, which also required the user to crop a rectangular region of interest containing the kidney. In another approach presented by Sun et al. [11], subpixel registration is considered where the problem is handled by energy minimization methods. In this energy minimization method, a subpixel motion model is used with temporal smoothness constraints.

For the segmentation problem, Yang et al. [4] divided the kidney into three regions of interest from the cortex and the outer medulla as 2×2 pixels manually and proposed a signal intensity analysis approach using autoregressive modelling. Sun et al. [12] suggested a level set and region growing based energy minimization approach to segment the cortex, medulla and pelvis structures.

At the final step of almost all the previous studies, either by manual pixel selection or by automatic segmentation, a particular location is selected from the cortex or the medulla, and the change of its gray level is tracked in time, resulting in a perfusion curve which will be explained in more details in sec. 3.3. This perfusion curve is the key

indicator of whether the kidney is performing its function or not as it shows the uptake and excretion of the contrast agent. However, as stated before, tracing the gray level changes at particular locations in the kidney is not a simple task due to the kidney motion and the low contrast of the typical dMRI sequences; thus, accurate segmentation and registration algorithms are required.

3. METHODS

In this paper we introduced a novel and automated technique (i) to segment the kidney and (ii) to correct for the motion artifacts caused by breathing and patient motion using Dynamic Contrast-Enhanced Magnetic Resonance Imaging. Our image analysis consists of three major steps, details of which will be given in the following sections:
• Segmentation of the kidney from dMRI scans using active contours. The external energy function of active contours has been modified to handle both shape models and gray level distributions.
• Motion compensation using an enhanced mutual information registration algorithm, and
• Evaluation of the kidney functionality via the perfusion curves.

3.1. *Step I. Segmentation*

Accurate segmentation of the kidney from dMRI is a challenge since the gray level distribution of the kidney and surrounding organs is not highly distinguishable, thus we employ statistical deformable models in the segmentation process. Our deformable model takes into account not only the gray level distribution but also a shape model of the kidney that depends on a sign distance map.

In conventional deformable models, surfaces move in the direction that minimizes an energy function that is composed of internal and external energy components as explained in [13]. This energy component is given as

$$E = E_{\mathrm{int}} + E_{\mathrm{ext}} = \int_{\tau \in T} \big(\xi_{\mathrm{int}}\big(\phi(\tau)\big) + \xi_{\mathrm{ext}}\big(\phi(\tau)\big)\big)d\tau \tag{1}$$

where $\xi_{\mathrm{int}}\big(\phi(\tau)\big)$ and $\xi_{\mathrm{ext}}\big(\phi(\tau)\big)$ denote the internal and external forces, respectively. Here the internal energy is

$$\xi_{int}\big(\phi(\tau)\big) = \alpha|\phi'(\tau)|^2 + \beta|\phi''(\tau)|^2 \tag{2}$$

where weights α and β control the curve's tension and rigidity, respectively, and $\phi'(\tau)$ and $\phi''(\tau)$ are the first and second derivatives of the deformable surface $\phi(\tau)$ with respect to the index of a contour point τ (see [13] for details). In this energy formulation, we have modified the external energy component, and we have formulated an energy function using the density estimations of two distributions: the sign distance map from shape models and the gray level distribution.

3.1.1. *Empirical Estimation of the Gray Level Density:*

For the estimation of the gray level density of the images, we assume that the empirical density comes from two classes: the kidney and the other tissues. The density of these two classes is estimated using our novel modified EM algorithm [14], and Levy distance is calculated between the estimated density and the empirical density as a measure of convergence to the correct density.

3.1.2. *Empirical Estimation of the Sign Distance Map Density:*

In order to obtain a shape model that describes the kidney, we used the dMRI data sets from the patients enrolled in this study. Our algorithm for extracting the 3D shape model of the kidney is as follows:

  (i) Align the collected data sets together using 3D rigid registration.

  (ii) Manually segment the kidney from the dMRI.

  (iii) Calculate the 3D edge V that describes the boundary of the kidney for each time sequence of dMRI.

  (iv) Calculate the average 3D surface shape V_m of the kidney, for N number of dMRI sequences by
    $V_m = \frac{1}{N}\sum_{i=1}^{N} Vi$

(v) Given a shape surface, define a function that describes the distribution of sign distance map inside and outside the shape as follows:

$$S(i,j) = \begin{cases} 0 & (i,j) \in V \\ d((i,j),V) & (i,j) \in R_V \\ -d((i,j),V) & Otherwise \end{cases} \qquad (3)$$

where R_v is the region which lies inside the shape and $d((i,j),V)$ is the minimum Euclidean distance between the image location (i,j) and the curve V.

(vi) Estimate the density of this average shape of the kidney using our modified EM approach [14]

3.1.3. *External Energy Component for Deformable Models:*

The last step in the sign distance map density estimation gives the gives the $p_s(S|k)$ component of our external force, whereas the density estimation of the gray level gives the $p(q|k)$ component, where $k = 1,2$ is the class label. Combining these two components, the deformable model is completely specified as:

$$\xi_{ext}\big(\phi(\tau)\big) = \begin{cases} -p(q|k)p_s(S|k)p(k) & \text{if } k = k^* \\ p(q|k)p_s(S|k)p(k) & \text{if } k \neq k^* \end{cases}$$

So the curve (snake) $\phi(\tau)$ as described in [13] moves through the spatial image domain to minimize the total energy and finds the image contours accurately. The segmentation results using this approach is given in the figure below.

Fig. 1. Segmentation Results

3.2. *Step II. Mutual Information Registration*

In DCE-MRI sequences, the registration problem arises because of the patient & breathing movements and the continuously but non-uniformly changing gray level values throughout the kidney. To overcome this problem, Mutual Information (MI) is a natural choice as it can align images from different modalities accurately and robustly [15]. Our registration approach is based on a modified version of the rigid registration using MI where we incorporate our segmentation results into the registration function as we explained in [16]. In this registration scheme, the binary segmentation results are used as label information, then the mutual information is calculated between two pixels only if their label information is equal as described in [16]. The registration results have been tested visually using checkerboard methods as given in Figure 3, and the smooth continuity on the boundaries has proven the accuracy of our approach. Using registration, we align all the dMRI sequences of a patient with the first sequence of images of the same patient, which enables us to track a given pixel's temporal change of gray level.

4

Fig. 2. Registration Results

3.3. *Step III. Evaluation of the Kidney Function by DCE-MRI*

The perfusion curve is a plot of the temporal gray level variation within the cortex of the kidney in the dMRI sequences. From the segmented and registered kidneys, we are selecting a window from the cortex manually and plotting the gray level at these points in the cortex as a function of the scanning sequence. As shown in Figure 4, in the perfusion curves, the intensity is low at the beginning, and as the bolus is washed out, the signal intensity starts to increase back to its original values. This property of the temporal signals is very important to detect the acute rejection. As it can be seen from the perfusion curves, the rejected kidney shows a delayed perfusion pattern compared with the accepted kidney because of the graft enlargement, and the intensity cannot reach the same level of the accepted kidney indicating that the bolus is not washed out totally.
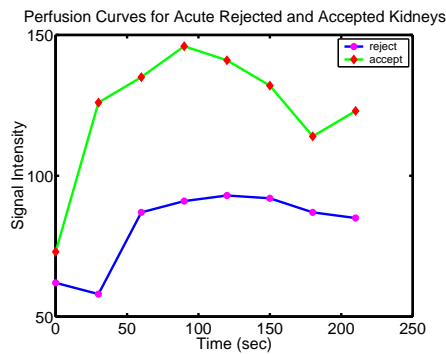

Fig. 3. Perfusion curve of a patient with biopsy proven acute rejection compared to an accepted kidney

4. RESULTS

In this study, gradient echo T1 imaging is employed by a Signa Horizon GE 1.5T scanner and the contrast agent Gadolinium DTPA is introduced via a wide bore veno-catheter placed at antecubital vein at a rate of 3-4 ml/sec with a dose of 0.2 ml/kg.BW. Images are taken at 5mm thickness with no interslice gap, repetition time (TR) 34 msec, field of view (FOV) 42x42 cm and the matrix is 256x160.

For each patient, 12 temporal sequences of coronal scans are taken, each sequence consisting of 6 images. The first image is taken at pre contrast, second image is at 0 second of injection and then the imaging is repeated every 30 sec for 10 times with the last image acquired 15 minutes after the start of injection.

In this paper, we introduced a new approach for the segmentation and registration of the kidney. The segmentation step used a model shape for the kidneys, and the density estimation of the sign distance map of this model shape as well as an estimate of the gray level distribution of the kidney is used to segment the kidney from the surrounding structures. The accuracy of our density estimation approach is calculated to be 0.008 using Levy distance method. Once the kidney is segmented in all the images, all sequences of a patient is registered onto the first time

sequence using rigid registration by the application of mutual information and global optimization algorithms. At the last step, a perfusion curve is plotted by tracing the points from the cortex of the kidney. The corresponding points in each sequence were obtained by maximizing the normalized cross correlation, which further reduced the effects of motion artifacts.

5. CONCLUSIONS

Kidney transplantation is a widely used method for the end-stage renal diseases, however, acute rejection still remains a problem and the early detection of the rejection using non-invasive techniques is a valuable approach. This paper introduced new methods in segmentation and registration for the detection of kidney rejection by means of Contrast Enhanced Dynamic Magnetic Resonance Imaging. Our proposed algorithm has been tested on several patients and it showed promising results compared to the manual segmentation of expert physicians.

However, because of the non-uniform behavior of the kidney in the contrast agent uptake, plots of the perfusion curves depend highly on the manual window selection and therefore discriminating the accepted and rejected kidneys has been left as an open question. Although the perfusion curves of accepted and rejected kidneys of two patients in Figure 3 are easily distinguishable, we haven't been able to come to a general solution in detecting acute rejection especially considering the fact that there are other diseases such as acute tubular necrosis or polyoma virus infection which look rejection. Therefore, our future work will include the evaluations of more patients to obtain a general pattern for the acute rejection via feature extraction from the signal curves and the training of Bayesian classifiers to automatically detect the successfully transplanted and rejected kidneys.

References

[1]   R.D.M. Allen and J.R. Chapman, *A manual of renal transplantation*. London: Edward Arnold, 1994, pp.127.

[2]   U.S. Department of Health and Human Services. Annual report of the U.S. scientific registry of transplant recipients and the organ procurement and transplantation network: transplant data: 1990-1999. Public Health Services, Bureau of Health Resources Department, Division of Organ Transplantation, Bethesda, MD; UNOS, Richmond, VA; 2000.

[3]   K. M. Rigg, "Renal transplantation: current status, complications and prevention," J Antimicrob Chemother 1995,36 Suppl: B51-B57.

[4]   D. Yang, Q. Ye, M. Williams, Y. Sun, T. C. C. Hu, D. S. Williams, J. M. F. Moura, and C. Ho., "USPIO-Enhanced Dynamic MRI: Evaluation of Normal and Transplanted Rat Kidneys," Magnetic Resonance in Medicine 46:1152-1163, 2001.

[5]   A. Fenster, D. B. Downey, and H. N. Cardinal, "Three dimensional ultrasound imaging", Topical Review, Phys. Med. Biol., 46, R67-R99, 2001.

[6]   P.L. Choyke, J.A. Frank, M.E. Girton, et al. "Dynamic Gd-DTPA-Enhanced MR imaging of the kidney: experimental results," Radiology 1989; 170:713-720

[7]   E.L.W. Giele, J.A. de Priester, J.A. Blom, J.A. den Boer, J.M.A. van Engelshoven, A. Hasman, and M. Geerlings, "Movement correction of the kidney in dynamic MRI scans using FFT phase difference movement detection," J. Magn Reson Imaging, Vol. 14, pp. 741-49, 2001.

[8]   P.J. Yim, H.B. Marcos, M. McAuliffe, D. McGarry, I. Heaton, and P.L. Choyke, "Registration of time-series contrast enhanced magnetic resonance images for renography," in Proc. 14th IEEE Symp. Computer Based Medical Systems, pp. 516-520, 2001.

[9]   G. Gerig, R. Kikinis, W. Kuoni, G.K. van Schulthess,and O. Kubler, "Semiautomated ROI analysis in dynamic MRI studies: Part I: image analysis tools for automatic correction of organ displacements," IEEE Trans. Image Processing, Vol. 11:(2),pp. 221-232, 1992.

[10]   Y. Sun, M. Jolly, and J. M. F. Moura, "Integrated Registration of Dynamic Renal Perfusion MR Images," ICIP'04, IEEE International Symposium on Image Processing, Singapore, October 24-27, 2004.

[11]   Y. Sun, J. M. F. Moura, C. Ho, "Subpixel Registration in renal perfusion MR image sequence," in Proc. 2004 IEEE Int. Symp. Biomedical Imaging, Arlington,VA, April 2004.

[12]   Y. Sun, J. M. F. Moura, D. Yang, Q. Ye and C. Ho, "Kidney Segmentation in MRI sequences using temporal dynamics," in Proc. 2004 IEEE Int. Symp. Biomedical Imaging, Washington,D.C.,July 2002.

[13]   M. Kass, A. Witkin, and D. Terzopoulos, "Snakes: Active contour models," *International Journal of Computer Vision*, vol. 1, pp. 321–331, 1987.

[14]   A. A. Farag, A. El-Baz, and G. Gimel'farb "Density Estimation Using Modified Expectation-Maximization for a linear combination of Gaussians", in Proc. IEEE Int. Conf. Image Processing (ICIP 2004), Singapore, October 2004.

[15]   J. B. West, J. M. Fitzpatrick, M. Y. Wang et al. "Comparison and evaluation of retrospective intermodality image registration techniques," J. Comput. Assisted Tomogr., vol. 21, pp. 554 -566, 1997.

[16]   A. El-Baz, S.E. Yuksel, S. Elshazly, A.A. Farag, "Non-rigid registration techniques for automatic follow-up of lung nodules" Computer Assisted Radiology and Surgery, CARS-05, Berlin, Germany, June 22-25, 2005 (accepted for publication).